CANADIAN JOURNAL OF EXPLORATION GEOPHYSICS
VOL. 29, NO. 1 (JUNE 1993), P. 266-275

ACOUSTIC ANISOTROPY OF DETERIORATED SOAPSTONE FROM THE NIDAROS CATHEDRAL, TRONDHEIM, NORWAY

RUNE M. HOLT[1], ANNE SKJÆRSTEIN[1] AND PER STOREMYR[2]

ABSTRACT

Partially severe deterioration has been observed in soapstones at the Nidaros Cathedral in Trondheim, Norway. Acoustic properties have been studied in order to develop a nondestructive technique for on-site quantification of the stone damage. The measurements show that sound velocities decrease strongly and also that the amount of anisotropy increases with increasing deterioration. These effects are related to two major orthogonal microcrack sets. In the most strongly deteriorated specimens, a shear-wave anisotropy between 50 and 100% was observed and for a given direction of propagation the faster *S*-wave had a higher velocity than the *P*-wave. The feasibility of acoustic techniques for mapping deterioration of monuments and buildings has been demonstrated.

INTRODUCTION

The original building period of the Romanesque and Gothic Nidaros Cathedral in Trondheim, Norway (Figure 1), terminated in the 13th century after a construction period of about 200 years (for a more detailed overview of the history and the geology of the Nidaros Cathedral, see Storemyr et al., 1992). The Cathedral was partly raised in the memory of King Olav Haraldsson, who was killed in the battle at Stiklestad (100 km north of Trondheim) in 1030. This historic event is thought to be the major single event leading to the christening of Norway. King Olav Haraldsson was probably buried at the site of the Nidaros Cathedral and became a saint, which has led to a large number of pilgrims coming from all over Europe to visit the Cathedral.

Today, through knowledge obtained during a continuing restoration effort, it has become evident that severe deterioration has occurred (see Figure 2) in sculptures, in the facades and in flying buttresses. Some of these elements are load-bearing structures. The main building stone of the cathedral is soapstone and it is in one particular type of this rock that the damage is significant.

The restoration of today involves mainly a replacement of damaged stones by freshly carved and sculptured stones. The selection of which stones to be replaced and which stones to be kept is currently based on experience and visual inspection only. There is a need for a more objective technique which may 1) quantify the amount of deterioration and 2) evaluate the penetration depth of damage within the stones.

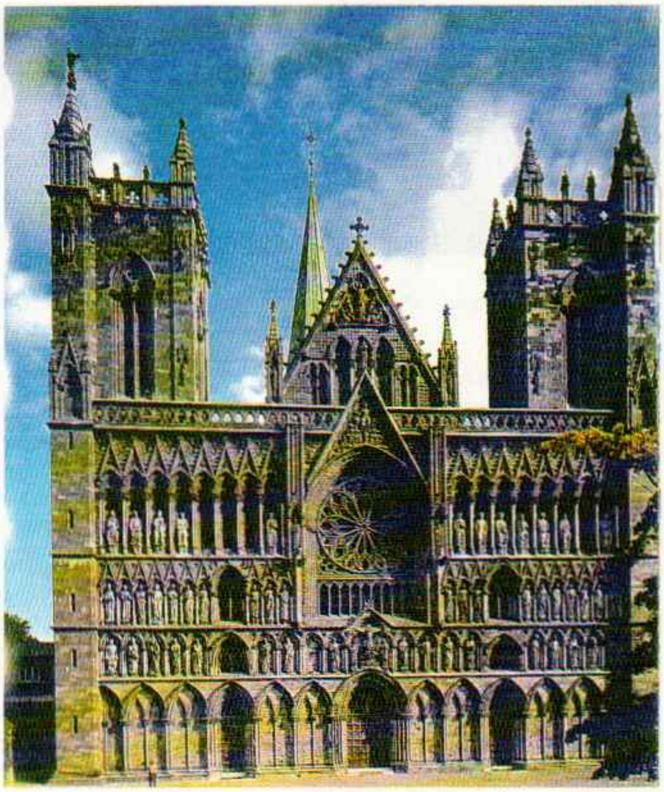

Fig. 1. The Nidaros Cathedral.

A research project was established to develop such a method. Since acoustic-wave propagation in rocks is known to be extremely sensitive to the presence of cracks (see, e.g., Fjær et al., 1992, ch. 6), a method based on acoustics was proposed as a possible solution to the on-site characterization. A similar attempt has been made by, for instance, Montoto et al. in their work with a spanish monastery (San Lorenzo de El Escorial, Madrid). A major step in the method-development phase was to characterize the soapstone

[1]IKU Petroleum Research/NTH Norwegian Institute of Technology
[2]SINTEF Rock and Mineral Engineering
This work has been supported financially by Conoco Norway Inc.

Fig. 2. Colour contrast between heavily deteriorated (brown/red/yellow) and less deteriorated (grey) soapstone on the outside wall of the Nidaros Cathedral. The intact (not deteriorated) soapstone is black in colour.

acoustically, in order to obtain a calibrated relationship between acoustic properties and deterioration. This paper will focus on the experimental results of the characterization study using samples taken from the cathedral. In a later stage of the project, true nondestructive testing (NDT) was performed on-site. This is briefly presented at the end of the paper.

Soapstone

The main building material of the Nidaros Cathedral is soapstone, which is a magnesium-rich, metamorphic rock type formed by the transformation of ultramafic and different magmatic or volcanic rocks (Wiik, 1953). The use of soapstone as a main building material has been largely restricted to Norway, where it is also found in other medieval churches (e.g., St. Mary's Church and Church of the Holy Cross in Bergen and Stavanger Cathedral). The availability of soapstone in Norway, as well as the fact that it is very easy to carve, are the major reasons for the predominant use of it in the Nidaros Cathedral. Before 1870, soapstones from two main quarries near Trondheim were used, while in the restoration work after that time as many as 20 different types of soapstone from all over Scandinavia have been used.

The soapstone studied here was quarried at Grytdal near Støren, about 50 km south of Trondheim. It is the stone type most prone to deterioration. XRD (X-ray diffraction) analysis shows that it is mainly composed of talc, chlorite, amphiboles (tremolite, actinolite), carbonates and sulphide minerals such as pyrite and pyrrhotite. Amphiboles are stiff, needle-shaped minerals which are visually observable particularly in the more deteriorated soapstones (see Figure 3). The amphiboles are mostly oriented with their long axis parallel to the foliation of the talc matrix. We have used this visible amphibole orientation as a reference for establishing the possible symmetry directions of the soapstone.

The causes of weathering are extremely complex and cannot be properly understood without careful investigations on actual facades and sculptures. Generally speaking, the most important reasons for the heavier deterioration of the Nidaros Cathedral are low-quality soapstone, low-quality mortars (Portland cement during restoration 1869 – ca. 1985), poor or damaged drainage systems in combination with the exterior climate and, to a minor extent, air pollution (Storemyr et al., 1992).

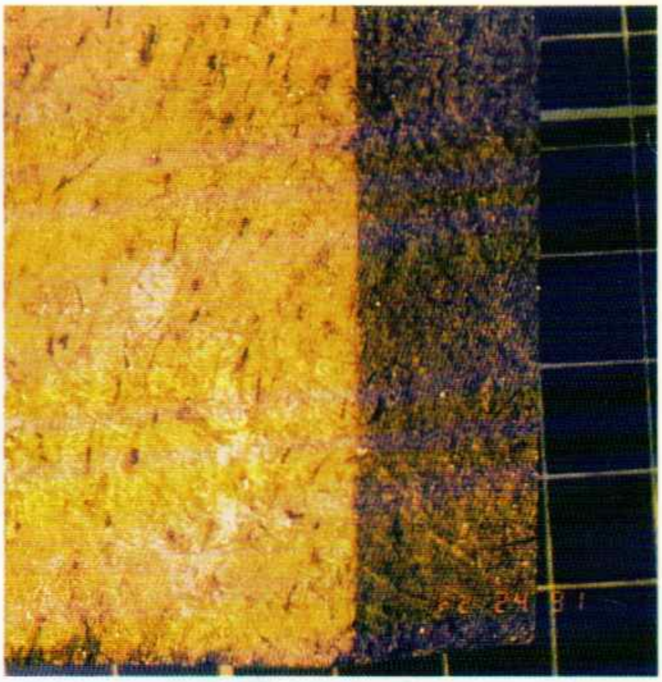

Fig. 3. Photograph of a deteriorated soapstone sample, showing the amphiboles as dark needle-like inclusions.

The presence of sulphur in the soapstone, in particular in the form of pyrrhotite, is undesirable as it enhances deterioration. This mineral may be poorly crystallized and susceptible to oxidation. Thus, gypsum and hygroscopic sulphates of magnesium may be formed when the released sulphate reacts with carbonates. The formation of such salts may initiate cracking and granular disintegration of the stones, because of the volume increase.

Experimental Methods

The methods described below all refer to laboratory characterization of soapstone samples. In-situ characterization is treated in a separate section towards the end of the paper.

Acoustic velocity measurements were performed by clamping two Panametrics broadband ultrasonic transducers (100-500 kHz frequency range) to opposite sides of the samples using a thin layer of glue (syrup) as a bonding agent. Both P- and polarized S-wave transducers were used. Figure 4a shows the experimental set-up, while Figure 4b shows examples of recorded wave trains. The measurement uncertainty depends on several factors including the length of sample determination, parallelism, reproducability of the gluing process and the force applied on the transducers to obtain good acoustic contact. In addition, the accuracy in picking arrival times, especially for shear waves, presents a problem. Normally, absolute values of velocities are expected to be correct within ±2-3% for *P*- and ±5-10% for *S*-waves. Notice in particular that the selected orientational symmetry and sample homogeneity attempted were verified by recording one wave train with cross-polarized shear transducers, then observing whether the shear-arrival amplitude is cancelled or not (i.e., perfect orientation and homogeneity should lead to cancellation).

A starting point, in order to obtain a calibration of acoustic velocities vs. deterioration, was to quantify deterioration by an independent petrophysical measurement. Two different methods, density and water absorption, were chosen for this purpose.

The density is reduced because of deterioration so that a low density implies a high degree of deterioration. Density measurements by volume and weight are easy and cheap to perform and were done for all samples in the set. Density measurements however are sensitive to errors in volume determination which here was done by measurement of side-wall lengths. A slightly irregular shape could result in significant error. Furthermore, heterogeneities in mineral distribution represents an additional source of error for the interpretation of deterioration.

Water absorption measurements give information about the interconnected porosity of the sample. Since it only measures pore space, it may be expected to provide a more direct measure of deterioration than the density. These measurements are more time-consuming and expensive than the density measurements.

Sample homogeneity is important for the value of the calibration. To check homogeneity, two different approaches were used. One is described above, namely the use of cross-polarized *S*-transducers. A second method utilizes x-ray tomography. Figure 5 shows examples of tomograms from an intact sample, a deteriorated sample and a sample containing a fracture not visible on the surface. The upper two tomograms show a striking difference between the intact and the deteriorated sample; the black dots present in the intact sample are most likely sulphides that are later dissolved during deterioration and therefore are absent in the deteriorated sample.

On the microscopic scale, samples were examined in a light microscope using thin sections. Also, fluorescence microscopy was used to image the spatial distribution of deterioration cracks.

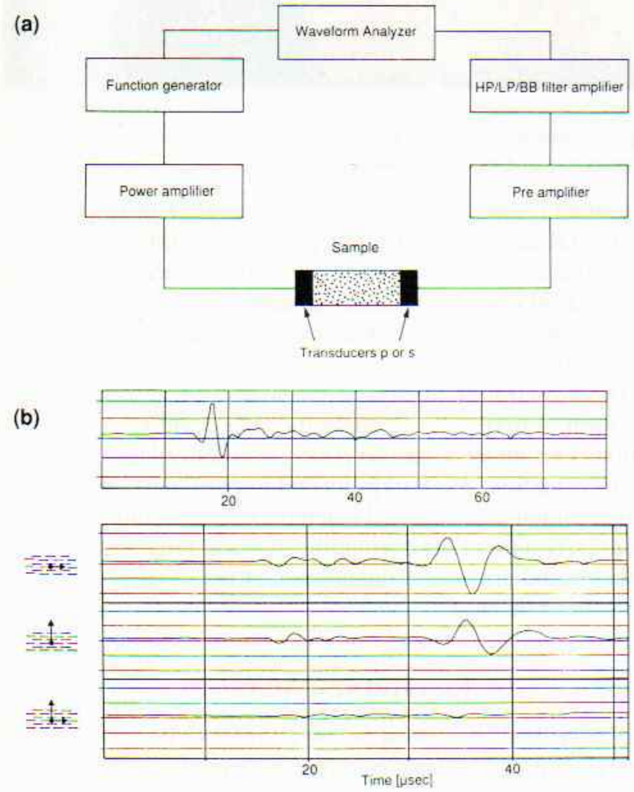

Fig. 4. (a) Sketch of the acoustic instrumentation set-up. The signals are generated by a WAVETEK function generator, fed through an ENI power amplifier into the transmitting PANAMETRICS transducer. After travelling through the sample as an acoustic wave, the pulse is converted to an electrical signal by an identical receiving transducer. It is then amplified by a PANAMETRICS preamplifier and further amplified and filtered by an adjustable highpass (HP)/lowpass (LP)/broadband (BB) WAVETEK filter-amplifier. Finally, the signal is recorded by a DATA 6000 waveform analyzer, which is also triggered by the function generator. **(b)** Typical waveforms obtained by transmission through a soapstone sample. Upper trace: *P*-wave signal; 2nd and 3rd trace: *S*-wave signals with orthogonal polarization and the same transmission path; bottom trace: *S*-wave signal with cross-polarized transducers (indicating sample homogeneity) (notice that the time scales on the *P*- and *S*-wave traces are different).

EXPERIMENTAL RESULTS

Introductory acoustic experiment

The first step in the method development was to identify to what extent the damage caused by deterioration could be seen by an acoustic wave. For this purpose, a 5-cm-thick cross-section was taken from the wall of the cathedral. The depth of the block (corresponding to the thickness of the wall near a window) was ~ 45 cm. This Grytdal soapstone sample was seen by visual inspection (by a yellowish colour) to be strongly deteriorated in a region near the outside surface while some major fractures could be seen near the inside.

Acoustic *P*-wave transmission through the block (parallel to the in situ facade, see Figure 6) identified a low-velocity zone in the outer 20-30 cm with a transition to a high-velocity zone deeper inside and a sharp decrease in velocity near the inner wall. The velocity structure corresponded to the colour contrasts and the fractured zones seen by the visual inspection.

This introductory test proved that acoustic velocities have the potential of identifying deterioration in this type of rock. It was further found that the amount of high frequencies present in the transmitted signals was lower in the deteriorated parts. Amplitudes are very uncertain but, in general, they seemed to be lower the more deteriorated the sample.

Characterization by nonacoustic methods

Following this test, a set of ≃ 20 cubic samples (≃ 5 x 5 x 5 cm^3) of Grytdal soapstone with various degrees of deterioration was selected for characterization. The samples were

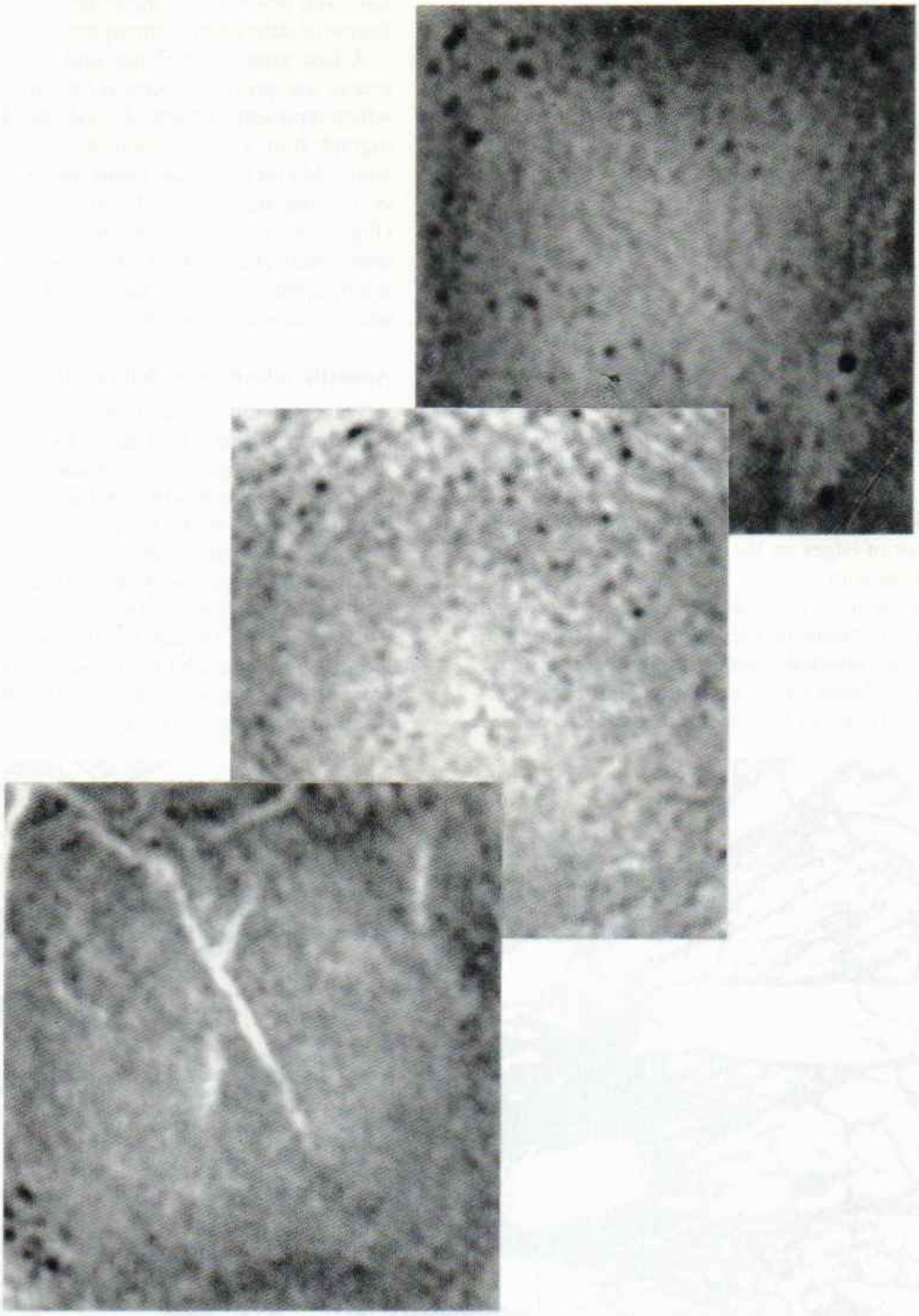

Fig. 5. X-ray tomograms (cross-sections) of intact (above), deteriorated (middle) and fractured (below) soapstones (these measurements were provided by the University Hospital in Trondheim).

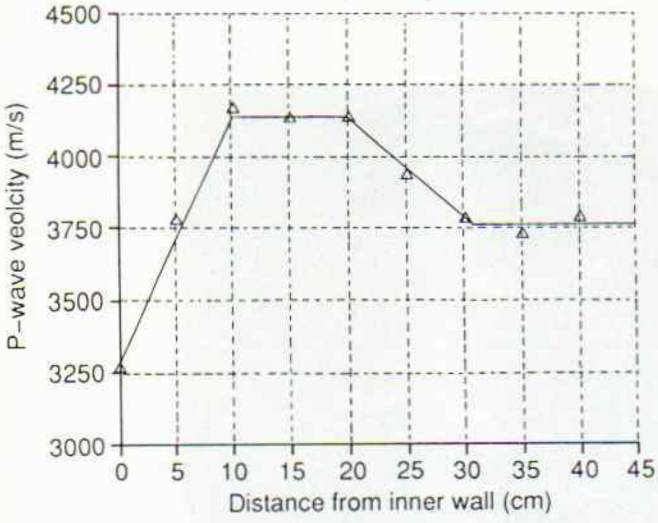

Fig. 6. *P*-wave velocity as a function of position within the wall, measured on a block of soapstone from the Nidaros Cathedral (wall thickness ~ 45 cm).

cut from a block that has been taken from the wall of the cathedral. One pair of edges on the cubes was parallel to the on-site surface of the wall.

Density and water absorption were measured to provide independent quantifications of the degree of deterioration. The densities of the selected samples varied between 2.61 and 2.87 g/cm^3 with lower values corresponding to the samples visually identified to be most deteriorated. Water absorption was determined with 10 samples, giving values from 0.7 to 2.6%. Since the porosity of soapstone normally falls well below 0.5%, these numbers clearly indicate a high degree of deterioration throughout the whole sample set.

A first assumption in our study was that the deterioration cracks are primarily *parallel* to the amphiboles/foliation, which represents a plane of weakness. Figure 7 shows a photograph from a thin section of a strongly deteriorated soapstone. Microcracks can easily be seen to have formed also *across* the amphiboles. Fluorescence microscopy analysis (Figure 8) seems to confirm the existence of two major orthogonal crack sets. Unfortunately, this technique could not be applied to all the samples. Also, no three-dimensional analysis was performed to check the full symmetry.

Acoustic velocities vs. deterioration

Wave velocities measured along the different axes of the cubes proved that the material exhibits acoustic anisotropy. Initially this anisotropy was assumed to be given mainly by a foliation associated with the rock fabric and measurements were performed on the basis of a transversely isotropic symmetry. The axis of symmetry (z direction, see Figure 9) was assumed to coincide with the normal to the predominant orientation of amphiboles. The x direction is chosen parallel to the long axes of the amphiboles, while the y direction is in the plane and parallel to the short axis of the amphiboles. Our initial assumption thus implied that the anisotropy of the intact soapstone is due to the foliation and that the

Fig. 7. Thin-section photograph from a deteriorated Grytdal soapstone sampled at the Nidaros Cathedral. Notice the cracks penetrating the amphibole grains.

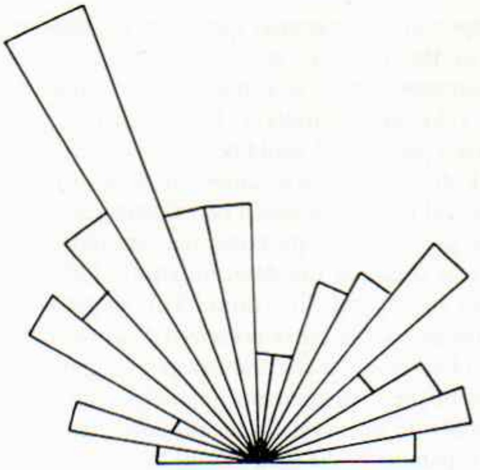

Fig. 8. Fluorescence microscopy images showing orientational distribution of microcracks in a deteriorated sample of Grytdal soapstone (these measurements were provided by the University of Oviedo, Spain).

amphiboles only serve as markers of the symmetry. Lack of truly intact (nondeteriorated) samples prevented this assumption from being verified. By observing the preferred orientation of the amphiboles, the assumed symmetry could be identified visually, in particular for deteriorated samples (see Figure 3). Sound velocity measurements were therefore performed with waves propagating in the assumed-symmetry (xy-) plane as well as at oblique angles to it. It was observed that the velocities of P- and S-waves propagating in the symmetry plane decreased with an increasing degree of deterioration (Figures 10, 11a). It was also observed that the velocities of two S-waves both propagating in the symmetry plane but with particle motions in (e.g., S_{yx}) and out (e.g., S_{yz}) of the plane were different. This is an example of shear-wave splitting or birefringence (Crampin, 1985). These two velocities are reduced an unequal amount with increased deterioration (Figure 11). It implies that the cracks formed during the deterioration process to a large extent have a preferred orientation. The in-plane polarized S-wave is always faster than that polarized out of the symmetry plane. The S-wave splitting observed here (Figure 11b) ranges from ~5 to 25%.

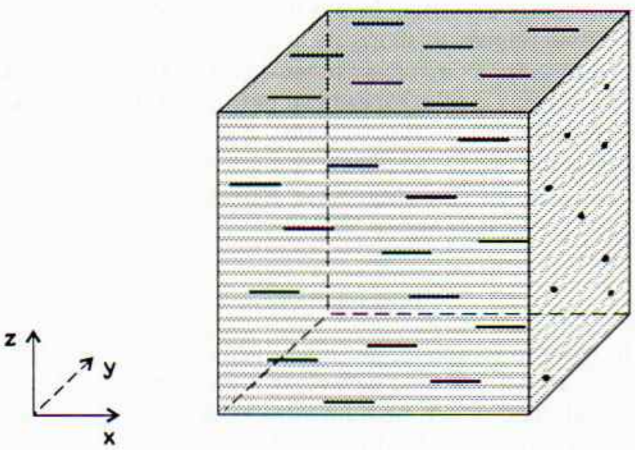

Fig. 9. Sample symmetry indicating foliation and amphiboles oriented with their long axis in the foliation plane. The x, y and z directions are shown in the figure.

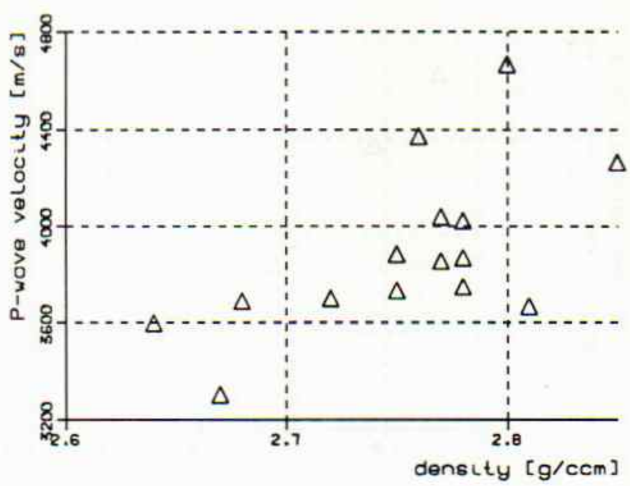

Fig. 10. P-wave velocity parallel to apparent symmetry plane (in the y direction) vs. bulk density.

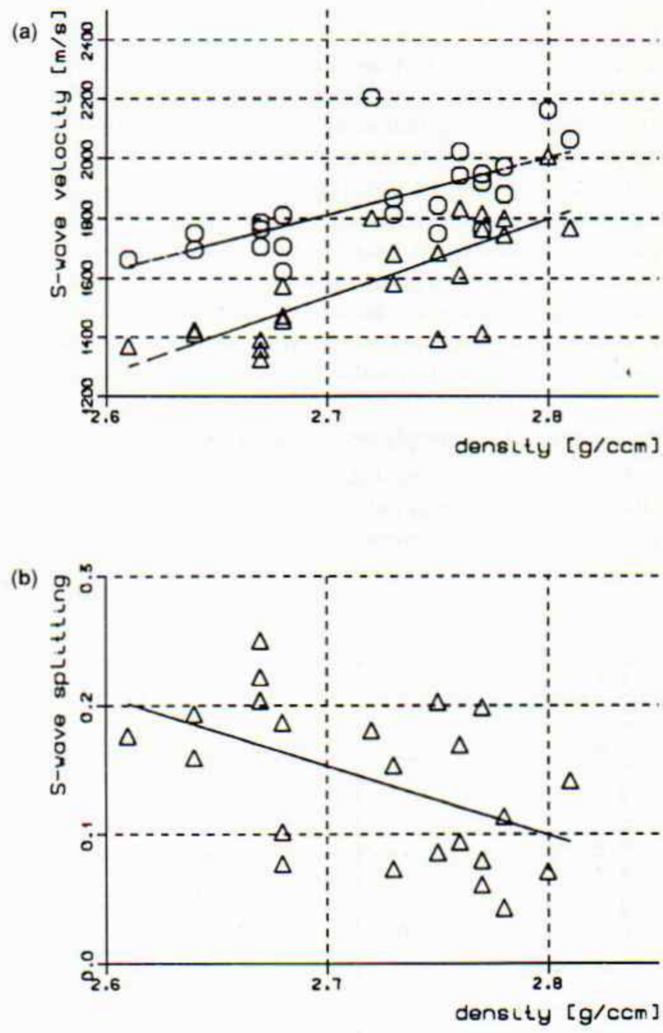

Fig. 11. (a) S-wave velocities vs. bulk density for propagation parallel to the apparent symmetry plane (in the y direction), polarized parallel (x) and perpendicular (z) to the same plane. o = S-wave parallel (v_{syx}); Δ = S-wave perpendicular (v_{syz}). **(b)** S-wave splitting (v_{syx} - v_{syz}) / v_{syz} vs. bulk density.

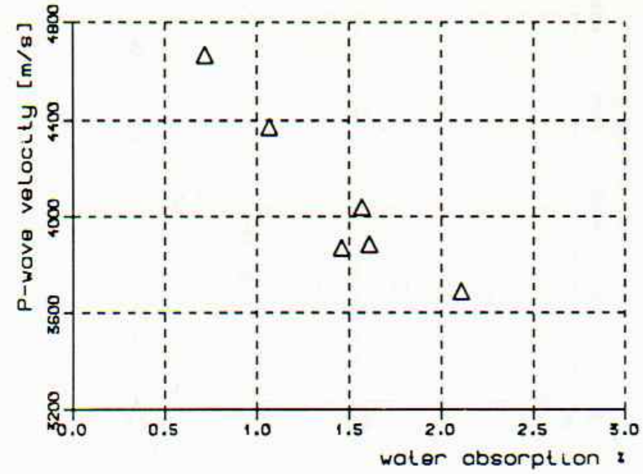

Fig. 12. *P*-wave velocity parallel to apparent symmetry plane vs. water absorption.

In Figures 10 and 11 the measured velocities were shown vs. density. In Figure 12, the water absorption is used as the deterioration parameter (for the samples where it was measured). The trend of decreasing velocity with increased deterioration seems more evident in this plot than in Figures 10 and 11, indicating that water absorption is probably a better measure of deterioration than density.

Further, the samples showing significant heterogeneity on the tomograms were removed from the data set in order to establish a correlation based only on homogeneous specimens. In addition, a check of homogeneity was added by measuring signal amplitudes with cross-polarized *S* transducers. The remaining set of samples shows a correlation between wave velocities and density as shown in Figure 13.

Anisotropy of a strongly deteriorated soapstone

Finally, one of the most deteriorated samples (with a density of 2.67 g/cm^3) was cut into a 10-sided prism, allowing a more detailed measurement of directionally dependent sound velocities.

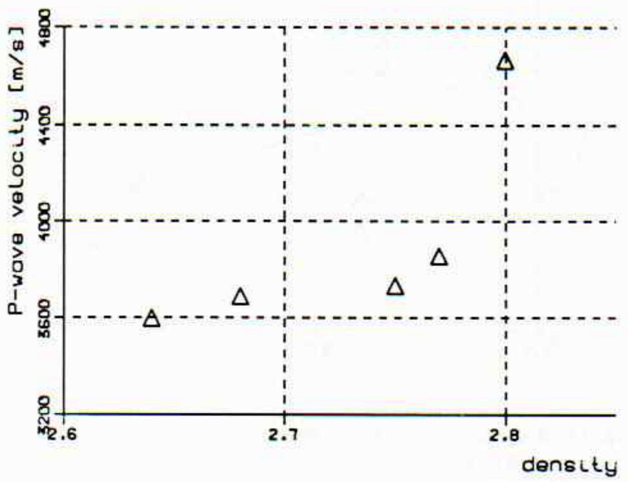

Fig. 13. *P*-wave velocity vs. density for a selected homogeneous set of samples.

For application in material quality evaluation, it is important to use the measured sound velocities to derive one or more parameters which is a more direct measure of damage than the velocities themselves. For the case of deterioration cracks, such parameters could be related to crack density and the crack distribution orientation. In order to see whether mathematical modelling based on effective medium theories could be used for this purpose, one strongly deteriorated sample was used for the determination of *P*- and *S*-wave velocities in several directions. This sample was found homogeneous by the cross-polarized *S*-wave method but it was not checked by x-ray tomography. Figure 9 gives the notations of the measurement geometry: the z direction is perpendicular to the (visually identified) plane of the amphiboles, x is parallel to the long axis of the amphiboles, while y is in the plane and parallel to the short axis of the amphiboles.

The *P*-wave velocities determined experimentally for the selected specimen were:

v_{px} = 1625 m/s,
v_{py} = 3365 m/s,
v_{pz} = 1145 m/s.

Notice here that the velocities in the assumed symmetry plane (xy) are indeed very different in such a deteriorated sample. The material, then, at most bears an orthorhombic symmetry. Notice also that the maximum *P*-wave anisotropy $(v_{py} - v_{pz})/v_{pz}$ is near 200%!

The *S*-wave velocities were (the indices denote propagation direction and polarization, respectively):

v_{syz} = 1315 m/s $\quad v_{szy}$ = 1420 m/s,
v_{sxz} = 1050 m/s $\quad v_{szx}$ = 905 m/s,
v_{syx} = 1720 m/s $\quad v_{sxy}$ = 1520 m/s.

The *S*-wave velocities should ideally be equal when propagation and polarization directions are interchanged. The fact that they are not may be related to measurement uncertainty but, nevertheless, indicate some heterogeneity, even though this sample was found to be quite homogeneous by x-ray tomography and the cross-polarized *S*-transducer studies.

Particularly interesting here is the wave propagation in the z direction. Figure 14 shows the waveforms recorded in this direction using *P*- and *S*-wave transducers. The velocity of the S_{zy}-wave is seen to exceed that of the P_z-wave, while the *S*-wave splitting [i.e., $(v_{szy} - v_{szx})/v_{szx}$)] is above 50%. Notice also that the *P*-wave amplitude is much lower than those of the two *S*-waves. The shear-wave anisotropy represented by $(v_{syx} - v_{szx})/v_{szx}$ is as high as 90%!

Interpretation

In order to recapture, our initial perception of the soapstone was that it should behave as a transversely isotropic material. The intact medium consists of a soft, foliated talc-rich matrix with hard needle-shaped inclusions (amphiboles) parallel to the foliation. During deterioration, we expected cracks to be formed in the foliation plane (plane of weakness). This would still lead to transverse isotropy.

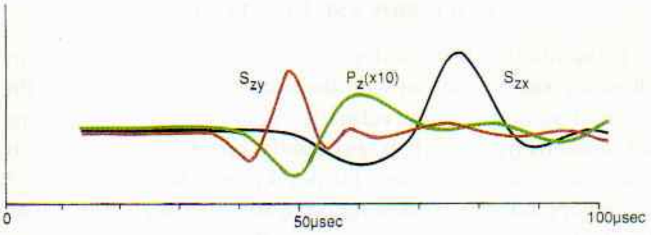

Fig. 14. Recorded S_{zy}, P_z (amplified 10x) and S_{zx} waveforms.

However, thin-section analysis (Figure 7), fluorescence microscopy (Figure 8) and acoustic-velocity measurements with a strongly deteriorated speciman indicated that two predominantly orthogonal crack sets are developed, one inside the soft matrix and the other through the hard inclusions. The symmetry of the medium is thus changed from transversely isotropic to orthorhombic. Clearly, in a more complete study, the full three-dimensional symmetry of the samples should be checked, both for the intact and the more deteriorated samples. The lack of truly intact samples of the Grytdal soapstone prevented this from being done here.

At our present level of investigation, we do not have sufficient parameters to allow detailed mathematical modelling. By assuming that the material consists of orthogonal crack sets in an isotropic matrix (orthorhombic symmetry) and estimating matrix parameters from our measurements in samples with low degrees of deterioration we used the theories of Hudson (1981) and Garbin and Knopoff (1973, 1975) to calculate the directionally dependent v_p and v_s values from two measured velocities. The theory of Hudson treats the cracks as a perturbation of the material stiffness and is not valid for high crack densities. In this case, this model confirms that the fast *S*-waves would be faster than the *P*-wave in the direction perpendicular to the plane of the major cracks (see the Appendix for an illustration of theoretical predictions with a single crack set). It, however, also predicts that the material would be unstable, since some of the elements in the stiffness matrix become negative. The theory of Garbin and Knopoff treats the cracks as a perturbation to the compliance of the material. Thus, the instability problem is avoided. In fact, the observed *P*-wave velocity anisotropy can be well-described by this model. However, the *S*-wave velocities are largely underestimated. In particular, for this model, the *S*-wave can never travel faster than the *P*-wave in any direction, contrary to the experimental indications (see Appendix).

It thus appears that no currently available theoretical model is able to handle a situation with the high crack density and high anisotropy observed in the most deteriorated samples.

Possible On-site Application

Pilot test at the Nidaros Cathedral

A pilot test has been performed at the Nidaros Cathedral investigating stones spanning a variety of deterioration states.

Fig. 15. Flying buttress from the Nidaros Cathedral showing a variety of deterioration states.

A flying buttress (Figure 15) has been studied in particular, since in this case the constituent blocks could be approached from more than one surface. This permitted measurements of *P*-wave velocities in transmission. The data could be integrated directly into a geological classification map of the cathedral.

Also, blocks within the main wall were investigated. For these measurements to be performed on the facade, the transmitting source as well as the receiver(s) therefore have to be placed on the same surface. Bulk *P*- and *S*-waves are generated and will propagate, depending on the transducer size and acoustic wavelength, in all directions from the source. Some of this energy will also hit the receiver as "direct *P*" and "direct *S*" arrivals. The bulk waves may also be reflected from outer surfaces of the structure (The Nidaros Cathedral consists of ashlars which are normally $\simeq 0.5 \times 0.5 \times 0.5$ m^3 in size) or from inner surfaces, like macroscopic fractures (> wavelength) or transition zones between low- and high-velocity material. In addition, a dominant mode of acoustic propagation with this geometry will be surface waves (Rayleigh waves). These are waves propagating along a free surface at a speed slightly lower than the shear-wave speed and with the wave energy confined within the upper ~ 1 wavelength. Thus, by varying the wavelength, i.e., the measurement frequency, it is feasible to obtain a measure of the shear-wave velocity vs. depth beyond the surface of a block. This is of interest for determination of the depth of penetration of a damaged zone. Notice that destructive actions such as extensive drilling of cores or holes could not be performed on-site and should not be part of the final technique.

For surface-wave excitation, a standard *P*-wave transducer was used with a wedge of a low-velocity material causing critical reflection of bulk *P*- and *S*-waves and (in principle) propagation only of the surface wave. Normally, measurements were taken with one source and 2-4 receiver positions along a given direction, with source-receiver distances varying from 10-25 cm. In order to map the anisotropy, similar measurements were performed in 2 or 3 additional directions. The result is a rosette of sound-velocity determinations, as exemplified in Figure 16. This measurement indicates a high degree of anisotropy. One complicating factor in the analysis is that the symmetry is unknown and can not be obtained by any independent means when only the rock surface is exposed. Introductory studies of the surface-wave velocity frequency dependence in a relatively narrow frequency range (30-50 kHz) did not indicate a strong variation of deterioration with depth (for this frequency range ~ 3 - 5 cm). Unfortunately, there was no independent means of checking this, since samples at this stage of the study could not be taken from the site for further study in the laboratory.

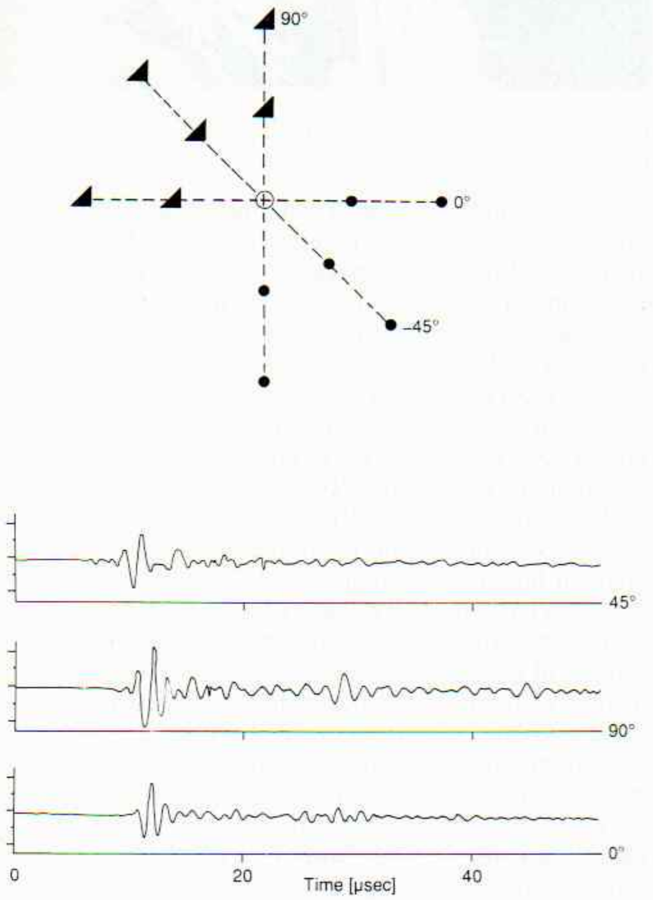

Fig. 16. Above: measurement configuration on a surface of a block on the Nidaros Cathedral. Triangles denote transmitters and circles are receiver positions. Spacings vary from 10 - 20 cm. Below: waveforms recorded for 10-cm propagation paths in 3 different directions, indicating anisotropy.

Discussion and Conclusions

In summary, the results of the acoustic measurements show a good correlation with the state of deterioration for the Grytdal soapstone; the velocities are strongly reduced and the anisotropy (which is extremely large) is enhanced by increasing deterioration. To our knowledge, such a high anisotropy has never been reported for a geological material. For instance, for wave propagation perpendicular to the predominant crack plane, *S*-wave splitting above 50% was observed in one case. Here also the fastest *S*-wave appears to travel faster than the *P*-wave and the maximum *P*-wave anisotropy is approximately 200%.

The indication that the symmetry may change when the material is transferred from its "intact" (transversely isotropic) to a deteriorated (orthorhombic) state makes the correspondence between deterioration and acoustic velocities rather complex. Also, no theoretical model is currently able to handle the extremely large anisotropy observed. On-site, only a few acoustic parameters can be obtained, and it is normally not possible to identify the symmetry. It will therefore be very difficult from such measurements to perform any inversion from velocities to crack density and crack orientation distribution.

An additional complicating factor is inferred by the heterogeneity of the soapstones, which is evident both at the short-length scale (where calibrations are obtained) and at longer length scale (where on-site testing is to be performed). This again means that the correlations found during calibration are at best valid only in an average sense and that the measurements on-site should be used only as qualitative indicators of deterioration damage.

The quality of the calibration depends not only on the acoustic measurements but also on the independent measure of deterioration to be calibrated against. For soapstones, water absorption (or effective porosity) seems to be the most relevant parameter, although others (like density) clearly could be used. Mineral composition by XRD (in our case, particularly pyrrhotite) or X-ray tomography are also potential classification techniques. Other possible measures are permeability or crack amount determined from, for instance, fluorescence microscopy.

A combination of techniques where both *P*-, *S*- and surface-wave velocities are obtained in a rosette (to indicate anisotropy) seems to be a good approach to evaluate the on-site deterioration properties. It remains to transform velocity and anisotropy magnitudes into a classification scheme, where the various blocks are assigned "colours" or descriptive terms like "severely damaged: should be replaced" (low velocities, high anisotropy) and "relatively intact: should be kept" (high velocities, low anisotropy). These criteria should be relatively easy to establish while the intermediate criteria requires more evaluation. This needs to be done in close cooperation with the end users, in this case the restoration workshop at the Nidaros Cathedral and preservation authorities in Norway.

One additional criterion that may arise is "uncertain condition: should be monitored again". This is one of the strengths of the acoustic measurement techniques — it will be fairly easy to repeat a set of measurements at a later stage (i.e., after one or two years) and then monitor quantitatively the change in the deterioration state. Similarly, using acoustic velocity measurements, possibly combined with acoustic emission measurements, as a research tool in accelerated laboratory studies of deterioration would be of value (Montoto et al., 1991).

The important question of finding the depth of penetration of deterioration damage has been addressed during this phase of the work. Clearly, the acoustic surface-wave technique has a potential for this.

A number of possible applications of this type of nondestructive testing (NDT) technique exists apart from the specific target of this study (the Nidaros Cathedral). In Europe, several cathedrals and monuments of the cultural heritage need detailed inspection to map existing damage and prevent further damage.

In summary, this work has demonstrated the feasibility of acoustic measurement techniques for monitoring rock deterioration.

REFERENCES

Crampin, S., 1985, Evaluation of anisotropy by shear-wave splitting: Geophysics **50**, 142-152.

Fjær, E., Holt, R.M., Horsrud, P., Raaen, A.M. and Risnes, R., 1992, Petroleum related rock mechanics: Elsevier Science Publ. Co., Inc.

Garbin, H.D. and Knopoff, L., 1973, The compressional modulus of a material permeated by a random distribution of circular cracks: Q. Appl. Math. **30**, 453-464.

______ and ______, 1975, The shear modulus of a material permeated by a random distribution of circular cracks: Q. Appl. Math. **33**, 296-300.

Hudson, J.A., 1981, Wave speeds and attenuation of elastic waves in materials containing cracks: Geophys. J. Roy. Astr. Soc. **64**, 133-150.

Montoto, M., Calleja, L., Perez, B. and Esbert, R.M., 1991, Evaluation in situ of the state of deterioration of monumental stones by non-destructive ultrasonic techniques: Proc. Mat. Res. Soc. Symp. **185**, 273-284.

Storemyr, P., Alnæs, L., Henriksen, J., Anda, O. and Waldum, A., 1992, Diagnosis for integrated conservation of the Nidaros Cathedral, Trondheim, Norway: Proc. 7th Internat. Congr. on Deterioration and Conservation of Stone, Lisbon, 1489-1498.

Wiik, H.B., 1953, Composition and origin of soapstone: Bull. Comm. Geol. Finl. **165**, 1-57.

APPENDIX

The observation of a shear wave travelling faster than a *P*-wave for a given direction of propagation can be predicted by the theory of Hudson (1981) for a single set of parallel cracks, whereas the theory of Garbin and Knopoff (1973, 1975) does not allow such a situation.

The former theory is based on a scattering approach, treating the cracks as a perturbation to the stiffness tensor **C**, i.e.,

$$\mathbf{C}_{ij} = \mathbf{C}^0_{ij}\,(1 - \mathbf{Q}_{ij}\varepsilon), \tag{A1}$$

where $\mathbf{C}^0$ is the stiffness tensor of the noncracked medium, ε is the crack density (number of cracks per unit volume multiplied by the average third power of the crack radius, for penny-shaped cracks) and **Q** is a perturbation matrix defined in Hudson (1981).

The Garbin-Knopoff theory is based on a static approach and treats the cracks as perturbations to the compliance, i.e.,

$$\mathbf{C}_{ij} = \mathbf{C}^0_{ij}\,(1 + \mathbf{Q}_{ij}\varepsilon)^{-1}. \tag{A2}$$

Neither of the theories are self-consistent, so they can not be expected to be valid for high-crack densities. Nevertheless, if we evaluate the ratio $\mathbf{C}_{33}/\mathbf{C}_{44}$ ($= v_{pz}^2/v_{szy}^2$) for an initially isotropic solid (with Poisson's ratio $\upsilon = 0.20$) as the crack density is increased, we find (Figure A1) that Hudson's theory predicts $\mathbf{C}_{33} < \mathbf{C}_{44}$ for a critical crack density ε_c (≈ 0.13). Hudson's theory however leads to instability (imaginary values of the sound velocity) if the crack density is increased further. This limiting crack density is ≈ 0.165 for the case shown in Figure A1. Figure A2 illustrates how the two limiting crack densities depend on Poisson's ratio of the solid matrix. Garbin and Knopoff's theory can never lead to such an instability but will not predict *P*-waves to travel slower than *S*-waves. Only for crack densities below 0.04 do the two theories predict the same behaviour.

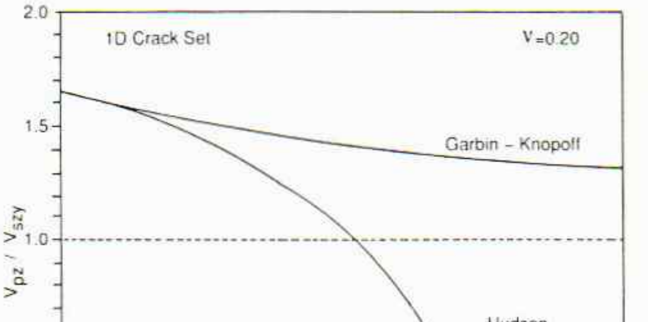

Fig. A1. The ratio of *P*- and *S*-wave velocities vs. crack density for propagation parallel to the crack normals for one single plane of cracks, according to Hudson's and Garbin and Knopoff's theories. Poisson's ratio of the intact solid $\upsilon = 0.20$.

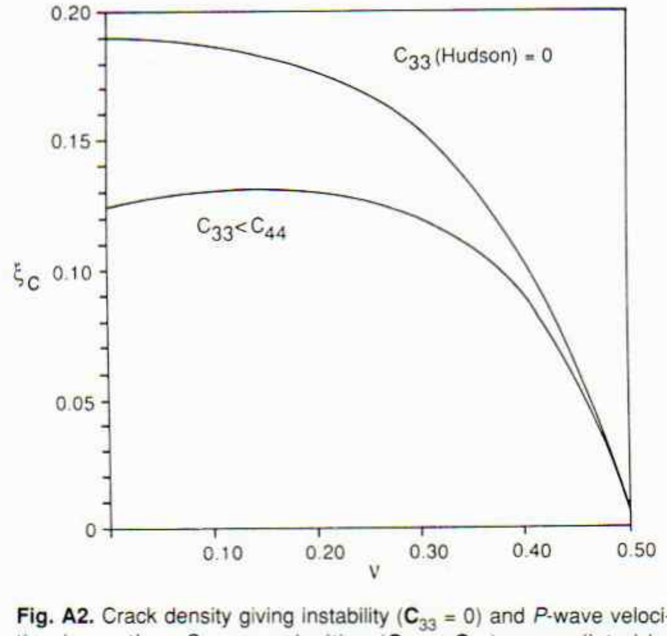

Fig. A2. Crack density giving instability ($\mathbf{C}_{33} = 0$) and *P*-wave velocities lower than *S*-wave velocities ($\mathbf{C}_{33} < \mathbf{C}_{44}$) as predicted by Hudson's theory.